Inorganic Chemistry

Article

pubs.acs.org/IC

Two New Dy_3 Triangles with Trinuclear Circular Helicates and Their Single-Molecule Magnet Behavior

Shuang-Yan Lin,[†,‡] Lang Zhao,[†] Yun-Nan Guo,[†,‡] Peng Zhang,[†,‡] Yang Guo,[†] and Jinkui Tang*[,†]

[†]State Key Laboratory of Rare Earth Resource Utilization, Changchun Institute of Applied Chemistry, Chinese Academy of Sciences, Changchun 130022, People's Republic of China

[‡]Graduate School of the Chinese Academy of Sciences, Beijing, 100039, People's Republic of China

Supporting Information

ABSTRACT: Self-assembly of polydentate Schiff base 2,6-diformyl-4-methylphenol di(benzoy1hydrazone) (H_3L), with dysprosium thiocyanate and sodium azide, affords two novel trinuclear triangular circular helicate dysprosium(III) complexes, $[Dy_3(\mu_3\text{-}OCH_3)_2(HL)_3(SCN)]\cdot 4CH_3OH\cdot 2CH_3CN\cdot 2H_2O$ (**1**) or $[Dy_3(\mu_3\text{-}N_3)(\mu_3\text{-}OH)(H_2L)_3(SCN)_3](SCN)\cdot 3CH_3OH\cdot H_2O$ (**2**), depending on the presence or absence of base. Single-crystal X-ray analyses show that two μ_3-methoxy oxygens cap the Dy_3 triangle in complex **1** and that one μ_3-OH and one μ_3-N_3^- cap the Dy_3 triangle of complex **2**, representing the first example of a μ_3-N_3^--capped lanthanide complex reported to date. Ac susceptibility measurements reveal that multiple relaxation processes and the onset of slow magnetization relaxation occur for complex **1** and **2**, respectively. Theoretical calculations are required to elucidate the underlying mechanism; however, the different magnetic anisotropy of the respective structures, which is dictated by the coordination environment of Dy^{III} ions and structural parameters of the triangles, is mostly responsible for the distinctive relaxation dynamics observed.

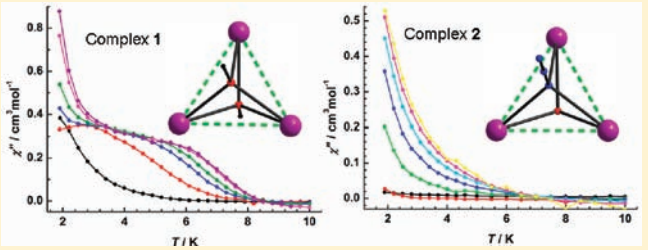

INTRODUCTION

Complexes exhibiting single-molecule magnets (SMMs) behavior, where relaxation and quantum tunneling of the magnetization is molecule-based, have attracted increasing interest[1] with the prospect of storing and processing magnetic information at a molecular level.[2] This interest has led to intense activity to consistently synthesize new molecular structures with a finite number of interacting magnetic centers suitable for detailed magnetic study. As a large number of SMMs emerged, understanding the factors determining the relaxation dynamics in such molecules becomes of primary importance with the goal of enhancing features such as the relaxation energy barrier compared with those of the originally studied examples.

Recent advances have shown that the synthesis of molecules containing heavy lanthanide ions, such as Tb^{III},[3] Dy^{III},[1a,c] Ho^{III},[4] and Er^{III}[5] ions with their highly anisotropic magnetic moments, is an important avenue to explore SMMs with higher anisotropic barriers. In fact, these elements have been responsible for many of the recent advances in SMMs, pushing the frontiers to longer relaxation times and higher temperature regimes.[3d,6] In addition to the well-established monometallic systems,[4a,5a,7] polynuclear Dy^{III} SMMs have become of increasing interest since the observation of the unusual slow relaxation behavior brought about by the toroidal arrangement of local magnetization vectors in a Dy_3 triangle.[8] Its unprecedented magnetic properties stimulate further investigation toward utilizing this highly anisotropic Dy_3 triangle as building blocks to create larger SMMs. Indeed, the opening up and linkage of such highly anisotropic dysprosium triangles in different forms have become a hot topic[6d,9] with the aim of creating new SMMs and possibly advancing the prospects of SMMs. Notably, the antiferromagnetical linkage of two Dy_3 triangles has been found to give a spectacular increase in the temperature at which slowing of the magnetization is observed from 8 K to 25 K.[6d]

With this in mind, we focus our attention toward a systematic survey of the structural types and characteristics of the resulting Dy_3 triangles through modifying the capping as well as surrounding ligands. We have prepared two new Dy_3 triangles, i.e., $[Dy_3(\mu_3\text{-}OCH_3)_2(HL)_3(SCN)]\cdot 4CH_3OH\cdot 2CH_3CN\cdot 2H_2O$ (**1**) and $[Dy_3(\mu_3\text{-}N_3)(\mu_3\text{-}OH)(H_2L)_3(SCN)_3](SCN)\cdot 3CH_3OH\cdot H_2O$ (**2**), by using polydentate Schiff base 2,6-diformyl-4-methylphenol di(benzoy1hydrazone) (H_3L). The crystal structural analyses demonstrate that both structures are triangular circular helicates. The triangle in **1** is capped by two μ_3-methoxy oxygens, while that in **2** is capped by one μ_3-OH and one μ_3-N_3^- bridge. Magnetic studies reveal the relaxation dynamics of **1** and **2** are drastically different. Indeed, the two maxima χ'' are indicative of the operation of more than one relaxation process in **1**, while only a temperature-dependent out-of-phase signal without peaks is observed in complex **2**. The distinct magnetic anisotropy reflected by the

Received: February 18, 2012
Published: April 17, 2012

different coordination environment of Dy^{III} ions in respective structures is most likely responsible for the significant magnetic disparities observed in these complexes.

EXPERIMENTAL SECTION

General Procedures. All starting materials were of A.R. Grade and were used as commercially obtained without further purification. 2,6-Diformyl-4-methylphenol (DFMP) was prepared according to a previously published method.[10] The Schiff-base ligand 2,6-diformyl-4-methylphenol di(benzoy1hydrazone) was prepared by the *in situ* condensation of 2,6-diformyl-4-methylphenol and benzoyl hydrazide in a 1:2 ratio in methanol/acetonitrile. Elemental analyses for C, H, and N were carried out on a Perkin-Elmer 2400 analyzer. Fourier transform IR (FTIR) spectra were recorded with a Perkin-Elmer FTIR spectrophotometer using the reflectance technique (4000−300 cm^{-1}). Samples were prepared as KBr disks. All magnetization data were recorded on a Quantum Design MPMS-XL7 SQUID magnetometer equipped with a 7 T magnet. The variable-temperature magnetization was measured with an external magnetic field of 1000 Oe in the temperature range 2−300 K. The experimental magnetic susceptibility data are corrected for the diamagnetism estimated from Pascal's tables and sample holder calibration.

X-ray Crystallography. Single-crystal X-ray diffraction measurements of the title complexes were carried out on a Bruker ApexII CCD diffractometer with graphite-monochromated Mo Kα radiation (λ = 0.71073 Å) at 185(2) K. The structures were solved by direct methods and refined on F^2 with full-matrix least-squares techniques using SHELXS-97 and SHELXL-97 programs.[11] The locations of Dy atoms were easily determined, and S, O, N, and C atoms were subsequently determined from the difference Fourier maps. Anisotropic thermal parameters were assigned to all non-hydrogen atoms. The H atoms were introduced in calculated positions and refined with a fixed geometry with respect to their carrier atoms. CCDC 852631 (**1**) and 852632 (**2**) contain the supplementary crystallographic data for this paper. These data can be obtained free of charge from the Cambridge Crystallographic Data Centre via www.ccdc.cam.ac.uk/data_request/cif.

Synthesis of $[Dy_3(\mu_3\text{-}OCH_3)_2(HL)_3(SCN)]\cdot 4CH_3OH\cdot 2CH_3CN\cdot 2H_2O$ (1). The complex was prepared by the reaction of $Dy(SCN)_3\cdot 6H_2O$ (104.6 mg, 0.24 mmol) with the H_3L formed by the *in situ* condensation of DFMP (25.5 mg, 0.15 mmol) and benzoyl hydrazide (41.7 mg, 0.3 mmol) in a 30 mL solution mixture of MeOH and CH_3CN (1:1, v:v) in the presence of KOH (0.3 mmol) and NaN_3 (13.5 mg, 0.2 mmol). The reaction mixture was stirred at room temperature for 2 h, and the resultant solution was left unperturbed. After a few days, orange, single crystals of complex **1** were obtained by slow evaporation of the solvent at room temperature. Yield: 21 mg, (13%, based on the metal salt). Anal. (%) Calcd for $Dy_3C_{80}H_{86}N_{15}O_{17}S$: C, 46.89, H, 4.23, N, 10.25. Found: C, 46.98, H, 4.03, N, 10.09. IR (KBr, cm^{-1}): 3176 (br), 3005 (w), 2853 (w), 2063 (m), 1624 (s), 1552 (s), 1517 (s), 1439 (m), 1378 (s), 1315 (m), 1231 (m), 1149 (w), 993 (w), 819 (w) 777 (m), 711 (s), 535 (w), 467 (w).

Synthesis of $[Dy_3(\mu_3\text{-}N_3)(\mu_3\text{-}OH)(H_2L)_3(SCN)_3]\cdot(SCN)\cdot 3CH_3OH\cdot H_2O$ (2). This complex was obtained by a similar procedure to that described for **1**, but without KOH. Yield: 28 mg, (16%, based on the metal salt). Analysis (%) Calcd for $Dy_3C_{76}H_{72}N_{19}O_{14}S_4$: C, 43.64, H, 3.47, N, 12.72. Found: C, 43.28, H, 3.18, N, 12.45. IR (KBr, cm^{-1}): 3414 (br), 3188 (w), 3006 (w), 2854 (w), 2069 (s), 1623 (s), 1573 (s), 1493 (w), 1445 (w), 1391 (m), 1329 (m), 1313 (m), 1233 (m), 1083 (w), 991 (w), 902 (w), 821 (w), 778 (m) 709 (m), 531 (w) 475 (w).

RESULTS AND DISCUSSION

The reaction of H_3L with dysprosium(III) thiocyanate and sodium azide in the presence of KOH in a mixture of methanol and acetonitrile (v/v = 1:1) produces complex **1** with the formula $[Dy_3(\mu_3\text{-}OCH_3)_2(HL)_3(SCN)]\cdot 4CH_3OH\cdot 2CH_3CN\cdot 2H_2O$ (**1**). A similar reaction, but in the absence of KOH, produces another Dy_3 cluster of formula $[Dy_3(\mu_3\text{-}N_3)(\mu_3\text{-}OH)(H_2L)_3(SCN)_3](SCN)\cdot 3CH_3OH\cdot H_2O$ (**2**). The use of KOH might promote the formation of μ_3-OCH_3 bridges; thus it is critical for the formation of complex **1**. Molecular structures of complexes **1** and **2** determined by single-crystal X-ray diffraction are depicted in Figure 1. Crystallographic data and refinement details are summarized in Table 1.

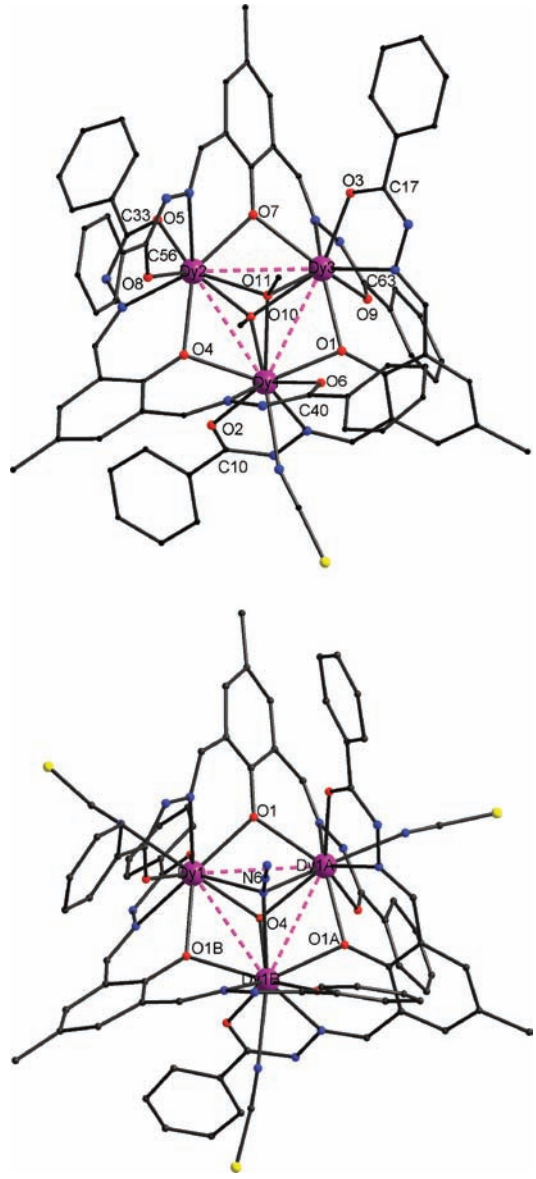

Figure 1. Structures of the Dy_3 triangular unit in **1** (top) and **2** (bottom) with selective numbering scheme. Hydrogen atoms have been omitted for clarity.

Complex **1** crystallizes in the monoclinic space group $P2_1/n$. The structure can be described as triangular circular helicate architecture,[12] which is twisted by three ligand strands along a pseudo-3-fold axis defined by the three metal ions of Dy1, Dy2, and Dy3. This triangular circular helicate structure is related to the rarely reported circular polymetallic lanthanide-containing helicates.[13] It is noteworthy that the triangle is capped by two μ_3-methoxy oxygens, instead of μ_3-hydroxo bridges as observed

dx.doi.org/10.1021/ic300371m | *Inorg. Chem.* 2012, 51, 10522−10528

Table 1. Crystal Data and Structure Refinement for Complexes 1 and 2

	1	2
empirical formula	$C_{80}H_{86}Dy_3N_{15}O_{17}S$	$C_{76}H_{72}Dy_3N_{19}O_{14}S_4$
fw (g/mol)	2049.20	2091.27
cryst syst	monoclinic	trigonal
space group	$P2_1/n$	$P\bar{3}$
cryst color	orange	yellow
a (Å)	15.0038(19)	19.4317(4)
b (Å)	30.470(4)	19.4317(4)
c (Å)	19.193(2)	15.3514(7)
β (deg)	94.460(2)	90
V (Å^3)	8747.7(19)	5020.0(3)
ρ_{calcd} (Mg/m^3)	1.556	1.384
$F(000)$	4084	2070
R_{int}	0.0531	0.0617
R_1, wR_2 [$I > 2\sigma(I)$]	0.0598, 0.1498	0.0639, 0.2015
R_1, wR_2 (all data)	0.0740, 0.1620	0.0958, 0.2303
GOF	1.113	1.069

in the prototype Dy_3[8a] and other Dy_3-related complexes.[6d,9a,b] Three edges of the triangle are bridged by three deprotonated phenoxide oxygen atoms of the ligands (O1, O4, and O7). Both Dy2 and Dy3 are coordinated by six O atoms and two N atoms of the ligands, exhibiting a distorted dicapped trigonal-prismatic coordinated arrangement, as shown in Figure S1. The coordination arrangement of Dy1 is a distorted tricapped trigonal-prismatic geometry filling the coordination sphere by an additional thiocyanato-N. This coordination sphere results in a less equilateral Dy_3 triangle, with Dy···Dy distances of 3.5762(6), 3.5838(6), and 3.5486(7) Å and Dy−Dy−Dy angles of 59.419(13)°, 60.397(11)°, and 60.184(11)°. The two μ_3-OCH_3 groups are displaced above and below the Dy_3 plane by 1.2320 and 1.2354 Å. The angles of μ_3-methoxy oxygen-bridged metal atoms are in the range 95.46(18)−96.67(19)°. The Dy−N and Dy−O distances are in the ranges 2.438(7)−2.596(7) and 2.273(6)−2.453(5) Å, respectively.

Complex **2** crystallizes in the trigonal space group $P\bar{3}$ and has a crystallographically centrosymmetric and therefore strictly equilateral triangle Dy^{III}_3 core. The structure shows three mono-deprotonated H_3L ligands wrapped around a genuine 3-fold axis defined by the three metal ions of Dy1, Dy1A (symmetry code A: $-x+y+1$, $-x+1$, z), and Dy1B (symmetry code B: $-y+1$, $x-y$, z), giving rise to a trinuclear circular helicate. It is interesting that the triangle of dysprosium centers is capped by one μ_3-OH and one μ_3-N_3^-, which represents the first example of a μ_3-N_3^--bridged lanthanide complex reported to date. Along each side of the triangle, a deprotonated phenoxido group of the ligand bridges two metal centers as in complex **1**. The triangle in **2** is equilateral with a Dy···Dy distance of 3.6314(8) Å. The environment of each Dy ion is N_4O_5 with a distorted tricapped trigonal-prismatic geometry (Figure S1). The μ_3-OH and μ_3-N_3^- are displaced above and below (1.1059 and 1.3573 Å) the Dy_3 plane with Dy−O−Dy angles of 99.991(1)° and Dy−N−Dy angles of 93.269(1)°. The Dy−N and Dy−O distances are in the ranges 2.452(9)−2.590(8) and 2.315(6)−2.437(6) Å, respectively.

As shown above, the existence of KOH promotes the deprotonation of the CH_3OH, resulting in two μ_3-OCH_3 caps in complex **1**. The ligands twisted along the central N−N bonds wrap around the Dy_3 plane, which gives rise to the circular helicate structures. Significantly, the configuration of the H_3L ligands imparts a coordination-induced chirality on each individual molecule, with the product crystallizing in an optically inactive 50:50 racemic mixture. Thus, both left- (Λ) and right-hand (Δ) configurations are clearly shown in both **1** and **2** at the metal plane, as observed in triple-stranded lanthanide helicate Ln_2 complexes.[14] The "meso" relation of the Λ and Δ configurations in the unit cell is clearly shown in Figures 2, 3, and S2.

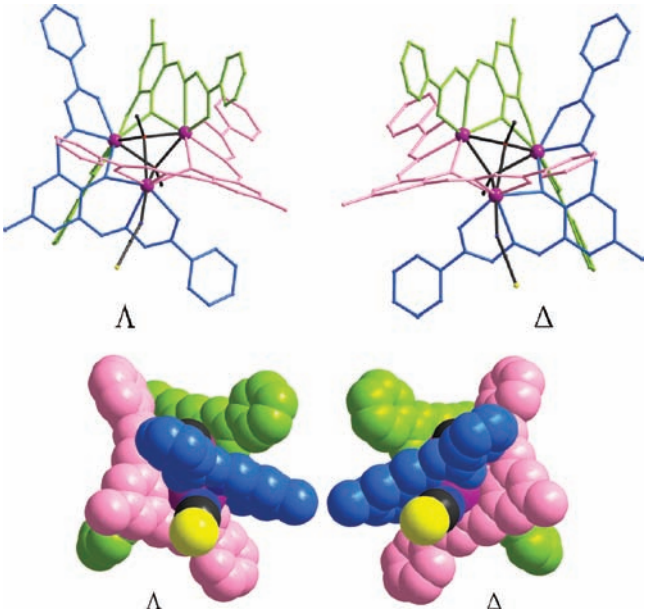

Figure 2. (Top) Schematic representations of left- (Λ) and right-hand (Δ) configurations of the trinuclear circular-helical structure in complex **1** with pseudo-C_3 axis. (Bottom) Space-filling representations of Λ and Δ helicates, showing the opposite helical arrangement of the ligands. Hydrogens are omitted for clarity, and the ligand strands are colored to emphasize the helicity.

Inspection of the intermolecular interactions in complex **1** shows that two lattice methanol molecules as hydrogen-bonding connectors join two Dy_3 units via strong O15−H15a···N5$^{\#4}$, O13−H13a···O15$^{\#3}$, and N12−H12···O13 (symmetry code: #3, $x+1/2$, $-y+1/2$, $z+1/2$; #4, $x-1$, y, $z-1$; Figure S3 and Table S1) hydrogen bonds; thus a 1D chain with a zigzag arrangement of the molecules is afforded. Such a chain disposes alternately Λ and Δ configurations of the molecules with the shortest intrachain Dy−Dy distance of 11.5907(12) Å. Obviously, the different enantiomers (Λ and Δ configurations) alternate throughout the network, as shown in Figure S4. Similarly, the packing arrangement for complex **2** also shows alternating Λ and Δ configuration layers along the a, b, and c axes with the shortest Dy···Dy distance of 9.5236(7) Å (Figure S5).

Magnetic Properties. The dc magnetic susceptibility studies of **1** and **2** were carried out in an applied magnetic field of 1000 Oe in the temperature range 300−2 K and plotted as $\chi_M T$ vs T (Figure 4). The two complexes show almost identical behavior within the margin of error. The observed $\chi_M T$ value at 300 K is 42.63 cm^3 K mol^{-1} for **1** (42.92 cm^3 K mol^{-1} for **2**), which is in good agreement with the expected value of 42.51 cm^3 K mol^{-1} for three uncoupled Dy^{III} ions (S = 5/2, L = 5, $^6H_{15/2}$, g = 4/3). Upon cooling, $\chi_M T$ gradually decreases until 50 K and then further decreases to reach a minimum of 21.19 cm^3 K mol^{-1} for **1** (14.85 cm^3 K mol^{-1} for

dx.doi.org/10.1021/ic300371m | Inorg. Chem. 2012, 51, 10522−10528

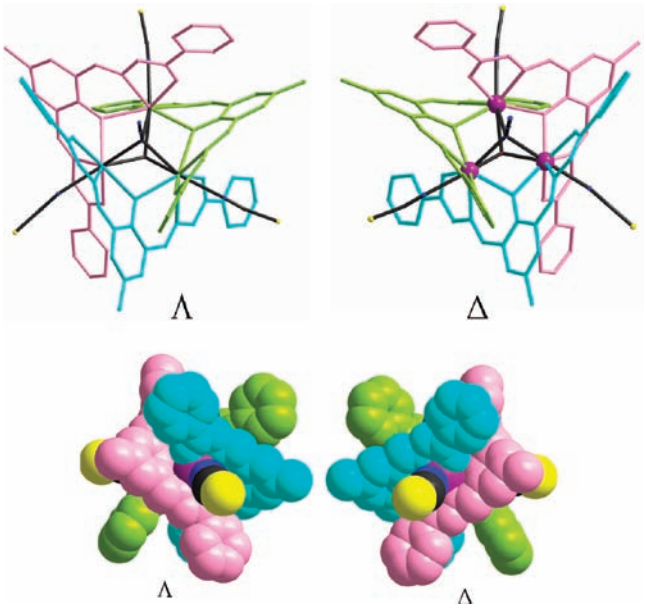

Figure 3. (Top) Schematic representations of left- (Λ) and right-hand (Δ) configurations of the trinuclear circular-helical structure in complex **2** with genuine C_3 axis. (Bottom) Space-filling representations of Λ and Δ helicates, showing the opposite helical arrangement of the ligands. Hydrogens are omitted for clarity, and the ligand strands are colored to emphasize the helicity.

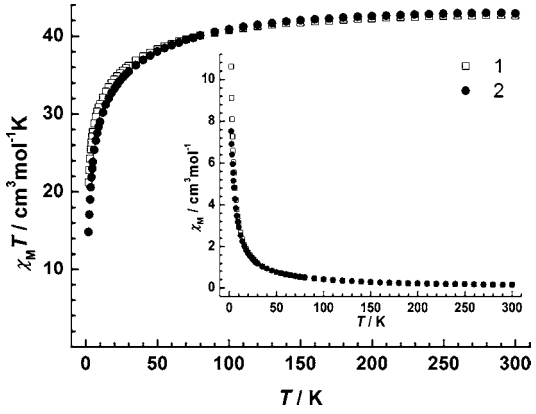

Figure 4. Temperature dependence of the $\chi_M T$ product and χ_M (inset) for **1** (open squares) and **2** (solid circles).

2) at 2 K. The susceptibility (inset of Figure 4) gradually increases with lowering the temperature and then dramatically increases to 10.61 cm^3 mol^{-1} at 2 K for **1** (7.44 cm^3 mol^{-1} for **2**). The decline in $\chi_M T$ is likely due to a combination of the progressive depopulation of Dy^{III} excited Stark sublevels[15] (Stark sublevels of the $^6H_{15/2}$ state) and possible exchange interaction between the metal ions.

Magnetization (M) data for **1** and **2** were collected in the field range 0−70 kOe below 5 K. The magnetization eventually reaches a value of 17.7 μ_B for **1** (17.3 μ_B for **2**) at 1.9 K and 70 kOe. This value is lower than the expected saturation value of 30 μ_B, but close to three uncorrelated Dy ions' magnetic moments (3 × 5.23 μ_B), which is likely due to crystal-field effects and the low-lying excited states.[16] Both the lack of saturation of the M versus H data and the nonsuperimposition of the M versus H/T data on a single master curve (Figure 5) suggest the presence of magnetic anisotropy and/or the lack of a well-defined ground state, where the low-lying excited states

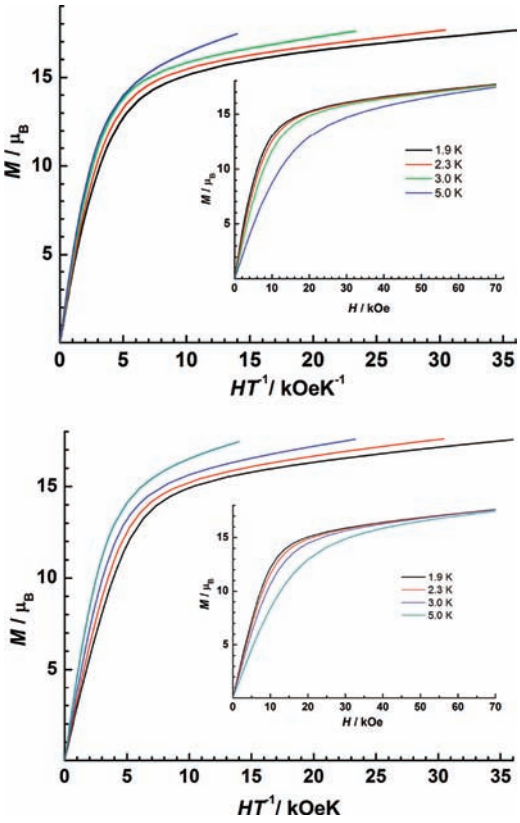

Figure 5. Plots of the reduced magnetization M vs H/T in the field range 0−70 kOe and temperature range 1.9−5.0 K. Inset: Field dependence of the magnetization. (Top) for **1**; (bottom) for **2**.

might be populated when a field is applied. At 1.9 K, the M versus H data of **1** exhibit slim butterfly-shaped hysteresis loops (Figure S6), without a remanence and a coercive field. This lack is due to the slow sweep rate of the loop compared with the fast zero-field relaxation,[17] while the M vs H hysteresis effect at 1.9 K was not found for complex **2** due to relatively faster relaxation process.

As shown above, $\chi_M T$ of both complexes at 2 K is quite far away from zero, and the magnetization at 1.9 K does not show any inflection in the low field; these tendencies indicate that both complexes are not nonmagnetic ground state, significantly different from the behavior of the prototype Dy_3.[8a]

Given the interesting magnetic behavior of the prototype Dy_3 triangle, the dynamics of the magnetization were investigated from the ac susceptibility measurements in the zero static field and a 3.0 Oe ac oscillating field. As shown in Figures 6, 7 and S7, an obvious temperature- and frenquency-dependent ac signal is detected for **1**, indicating slow relaxation of magnetization expected for a single-molecule magnet. The $\chi''(T)$ plot shows a broad shoulder between 2 and 8 K in the range 100−1200 Hz and a tail of the peak below 2 K. The nonvanishing of ac susceptibility at low temperatures is indicative of quantum tunnelling of the magnetization often seen in lanthanide SMMs.[5c,18] Furthermore, the $\chi''(\nu)$ plot clearly shows the occurrence of two distinct peaks in the out-of-phase ac signals, which demonstrates the possible occurrence of two relaxation processes. For instance, the χ'' versus frequency plot at 1.9 K clearly evidences two peaks, which are centered at 10 and 570 Hz, respectively. In contrast, the prototype Dy_3 shows a unique set of peaks.[8a]

dx.doi.org/10.1021/ic300371m | Inorg. Chem. 2012, 51, 10522−10528

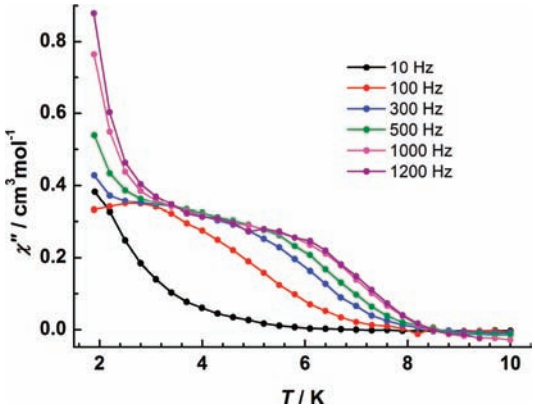

Figure 6. Temperature dependence of the out-of-phase (χ'') ac susceptibility for **1**. The solid lines are guides for the eyes.

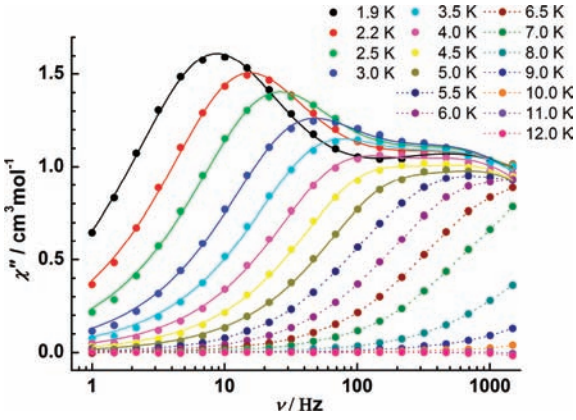

Figure 7. Frequency dependence of the out-of-phase ac susceptibility for **1** at H_{dc} = 0 Oe. The solid lines indicate the fits to eq 1. The dotted lines are guides to the eye.

To better understand the nature of both types of dynamics, the experimental $\chi_{ac}(\omega)$ curves between 1.9 and 5.0 K are simulated by the sum of two modified Debye functions[1e] (eq 1) and depicted as the $\chi'(\nu)$, $\chi''(\nu)$, and Cole−Cole plots in Figures S7, 7, 8, and S8, respectively. The relaxation times (τ) for each process derived from the two peaks of frequency-dependence data are plotted as a function of $1/T$. The effective energy barriers obtained by modeling the behavior with the Arrhenius law ($\tau = \tau_0 \exp(U_{eff}/kT)$) are 4.4 and 8.9 K and pre-

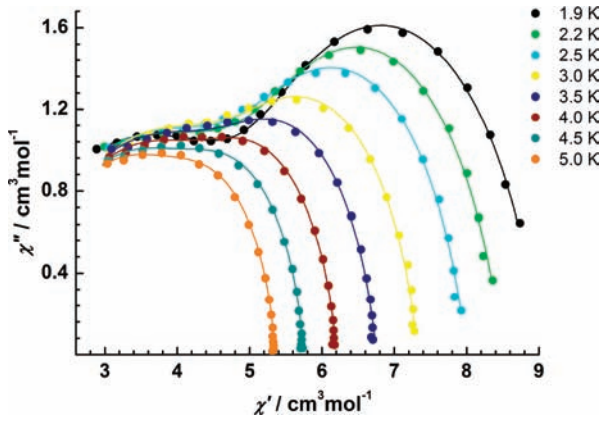

Figure 8. Cole−Cole diagrams for **1** between 1.9 and 5.0 K at zero-dc field, with the best fits to eq 1 given as solid lines.

exponential factors (τ_0) of 4.4×10^{-5} and 8.9×10^{-5} s for the FR (FR, fast relaxation phase corresponds to the high-frequency peaks) and SR (SR, slow relaxation phase corresponds to the low-frequency peaks), respectively (Figure S9). Below 3 K the relaxation times for the FR deviate from Arrhenius behavior, becoming temperature independent with a τ_{QTM} value of 2×10^{-4} s. It should be noticed that τ_0 are relatively larger than the expected values around 10^{-6}−10^{-11} s for SMMs. These values are obviously enhanced by the presence of QTM.

$$\chi_{AC}(\omega) = \chi_{s,tot} + \frac{\Delta\chi_1}{1 + (i\omega\tau_1)^{(1-\alpha_1)}} + \frac{\Delta\chi_2}{1 + (i\omega\tau_2)^{(1-\alpha_2)}} \quad (1)$$

The Cole−Cole plots (Figures 8 and S8) show two well-separated relaxation phases at low temperature and an asymmetric semicircle at high temperature (Figure S10). That is, the Cole−Cole plots go through an evolution from FR to SR at the frequency range of the test with increasing temperature. The two separate relaxation processes are clearly observed at 1.9 and 2.2 K (Figure S8), which can be nicely described by eq 1 with α parameters in the range 0.1−0.4.

For complex **2**, an obvious temperature-dependent ac signal (Figures 9 and S11) is observed below 7 K, indicating the onset

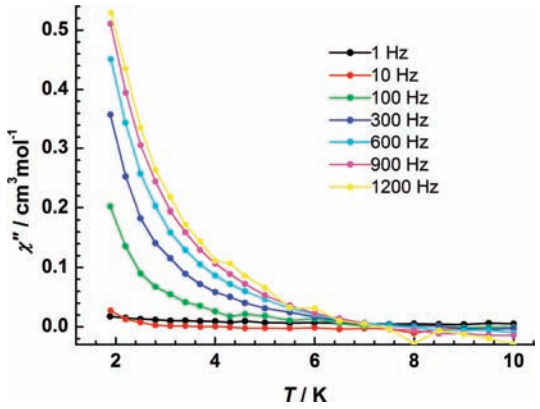

Figure 9. Temperature dependence of the out-of-phase ac susceptibility for **2** under a zero-dc field.

of slow magnetization (M) relaxation and, thus, probable SMM behavior. Unluckily, slow relaxation of magnetization for this complex is experimentally observed only over a short range of temperature, and no maximum of χ'' is observed in the temperature window technically available; thus we cannot determine the energy barrier and corresponding relaxation time. Alternatively, a method recently employed by Bartolomé et al.,[19] assuming that there is only one characteristic relaxation process of the Debye type with one energy barrier and one time constant, can be used to evaluate roughly the energy barrier and τ_0 based on the following relation (eq 2):

$$\ln(\chi''/\chi') = \ln(\omega\tau_0) + E_a/k_BT \quad (2)$$

This method has been applied earlier in the determination of the Mn_{12} acetate[20] and Dy_2 complex.[15c] As shown in Figure 10, by fitting the experimental χ''/χ' data to eq 2, we extract an estimate of the activation energy of ~3 K and the characteristic time of 10^{-6} s. A more precise result must wait for very low-temperature measurements (T < 1 K) by using a micro-SQUID.

dx.doi.org/10.1021/ic300371m | Inorg. Chem. 2012, 51, 10522−10528

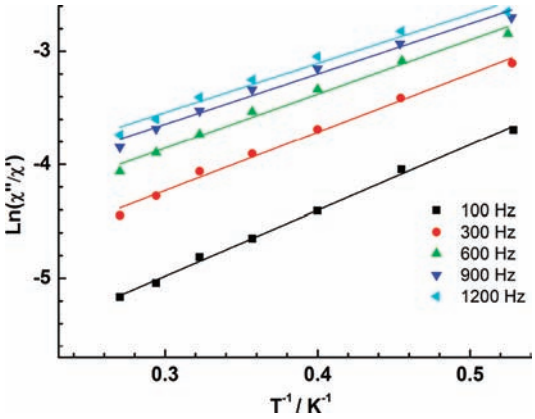

Figure 10. Plot of natural logarithm of χ''/χ' versus $1/T$ for **2**. The solid line represents the fitting results over the range 100−1200 Hz.

Although the dc magnetic susceptibilities of the two title Dy_3 triangles are very similar, their dynamic behaviors are dramatically different. It has been increasingly identified that the relaxation of magnetization in most polynuclear lanthanide clusters is presumably attributed to the large intrinsic magnetic anisotropy of 4f ions,[18b,21] due to very weak magnetic coupling between metal centers as a result of the efficient shielding of the unpaired electrons in their 4f orbitals.[22] It is also well-known that magnetic relaxation is extremely sensitive to tiny distortions of the coordination geometry. Therefore, the difference in the relaxation dynamics of **1** and **2** is probably due to the distinct coordination environments around the Dy^{III} ions, which are likely to affect the nature or directions of the easy axes through the ligand fields.[15c,18b,23]

Complex **1** contains two distinct metal centers, with nine-coordinate Dy1 in a distorted tricapped trigonal-prismatic arrangement and an eight-coordinate Dy2/Dy3 center in a distorted bicapped trigonal-prismatic geometry. The multiple relaxation processes observed are most likely associated with these distinct anisotropic centers. While in complex **2** all three Dy^{III} ions are the same nine-coordinate with a distorted tricapped trigonal-prismatic geometry, in contrast, Dy^{III} ions in the prototype Dy_3[8a] are all eight-coordinate. Hence, differences of coordination environment of Dy^{III} ions in the title complexes and the prototype Dy_3 result in the different symmetry and strength of the local ligand field of the Dy^{III} ions, which may strongly affect the magnetic anisotropy, thus causing distinct dynamic behavior.[23a,24] In addition, the weak magnetic interactions between the metal centers induced by the different u_3-caps might generate dissimilar anisotropy of lowest exchange multiplets, therefore affecting the dynamic magnetic behavior of the respective structure. The observed slow relaxation of the magnetization may arise from ground-state doublets of large $|M_J|$ values (such as 15/2 or 13/2), which can achieve an easy axis of the magnetization. However, further in-depth studies as well as *ab initio* calculations are required to get a conclusive answer on this point.

All in all, these features clearly suggest that the strength of the local crystal field modulated by different μ_3-bridges, the versatile H_3L ligand, and the auxiliary ligand (SCN^-) is responsible for the different magnetic dynamic behaviors observed, highlighting the possibility of tuning the magnetic properties of SMMs.

CONCLUSIONS

Two novel triangular circular-helicate Dy^{III}_3 complexes have been synthesized using the versatile hydrazone ligand H_3L. The helicates of the molecular unit are induced by the coordination of the twisted diazine bridges from H_3L ligands. Unlike the μ_3-OH-capped prototype Dy_3 triangle reported before,[8a] the Dy_3 triangle of complex **1** is capped by two μ_3-methoxy oxygens, while the triangle of complex **2** is capped by one μ_3-OH and one μ_3-N_3^- linkage. As far as we know, this is the first example of a μ_3-N_3^--bridged lanthanide complex reported to date.

Magnetic properties reveal that two maxima χ'' in complex **1** are indicative of the operation of more than one relaxation process in this compound, while only a temperature-dependent out-of-phase signal without peaks is observed in complex **2**. The significant magnetic disparities may be associated with the distinct anisotropic centers due to coordination-sphere differences of the metal centers. This presents an opportunity to tune the magnetic properties of SMMs by modifying the ligands and further adjusting the corresponding symmetry of the ligand field. Theoretical studies are required to thoroughly analyze the structural and magnetic property relationship of Dy_3 triangles.

ASSOCIATED CONTENT

Supporting Information

Tables of hydrogen bonds (Table S1) and figures of crystal structures (Figures S1−S5) and magnetic measurements (Figures S6−S11). This material is available free of charge via the Internet at http://pubs.acs.org.

AUTHOR INFORMATION

Corresponding Author

*E-mail: tang@ciac.jl.cn.

Notes

The authors declare no competing financial interest.

ACKNOWLEDGMENTS

We thank the National Natural Science Foundation of China (Grants 91022009 and 20921002) for financial support.

REFERENCES

(1) (a) Sessoli, R.; Powell, A. K. *Coord. Chem. Rev.* **2009**, *253*, 2328. (b) Wang, B. W.; Jiang, S. D.; Wang, X. T.; Gao, S. *Sc. China. Ser. B* **2009**, *52*, 1739. (c) Sorace, L.; Benelli, C.; Gatteschi, D. *Chem. Soc. Rev.* **2011**, *40*, 3092. (d) Rinehart, J. D.; Long, J. R. *Chem. Sci.* **2011**, *2*, 2078. (e) Guo, Y.-N.; Xu, G.-F.; Guo, Y.; Tang, J. *Dalton Trans.* **2011**, *40*, 9953. (f) Lin, S.-Y.; Guo, Y.-N.; Xu, G.-F.; Tang, J. *Chin. J. Appl. Chem.* **2010**, *27*, 1365.

(2) (a) Leuenberger, M. N.; Loss, D. *Nature* **2001**, *410*, 789. (b) Hill, S.; Edwards, R. S.; Aliaga-Alcalde, N.; Christou, G. *Science* **2003**, *302*, 1015.

(3) (a) Ishikawa, N. *J. Phys. Chem. A* **2003**, *107*, 5831. (b) Ishikawa, N.; Sugita, M.; Ishikawa, T.; Koshihara, S.; Kaizu, Y. *J. Am. Chem. Soc.* **2003**, *125*, 8694. (c) Takamatsu, S.; Ishikawa, T.; Koshihara, S.; Ishikawa, N. *Inorg. Chem.* **2007**, *46*, 7250. (d) Rinehart, J. D.; Fang, M.; Evans, W. J.; Long, J. R. *J. Am. Chem. Soc.* **2011**, *133*, 14236.

(4) (a) Ishikawa, N.; Sugita, M.; Wernsdorfer, W. *J. Am. Chem. Soc.* **2005**, *127*, 3650. (b) Blagg, R. J.; Tuna, F.; McInnes, E. J. L.; Winpenny, R. E. P. *Chem. Commun.* **2011**, *47*, 10587.

(5) (a) AlDamen, M. A.; Clemente-Juan, J. M.; Coronado, E.; Martí-Gastaldo, C.; Gaita-Ariño, A. *J. Am. Chem. Soc.* **2008**, *130*, 8874. (b) AlDamen, M. A.; Cardona-Serra, S.; Clemente-Juan, J. M.; Coronado, E.; Gaita-Ariño, A.; Martí-Gastaldo, C.; Luis, F.; Montero,

O. *Inorg. Chem.* **2009**, *48*, 3467. (c) Jiang, S. D.; Wang, B. W.; Sun, H. L.; Wang, Z. M.; Gao, S. *J. Am. Chem. Soc.* **2011**, *133*, 4730.
(6) (a) Lin, P.-H.; Burchell, T. J.; Ungur, L.; Chibotaru, Liviu F.; Wernsdorfer, W.; Murugesu, M. *Angew. Chem., Int. Ed.* **2009**, *48*, 9489. (b) Guo, Y.-N.; Xu, G.-F.; Gamez, P.; Zhao, L.; Lin, S.-Y.; Deng, R. P.; Tang, J.; Zhang, H. J. *J. Am. Chem. Soc.* **2010**, *132*, 8538. (c) Rinehart, J. D.; Fang, M.; Evans, W. J.; Long, J. R. *Nat. Chem.* **2011**, *3*, 538. (d) Hewitt, I. J.; Tang, J.; Madhu, N. T.; Anson, C. E.; Lan, Y.; Luzon, J.; Etienne, M.; Sessoli, R.; Powell, A. K. *Angew. Chem., Int. Ed.* **2010**, *49*, 6352. (e) Blagg, R. J.; Muryn, C. A.; McInnes, E. J. L.; Tuna, F.; Winpenny, R. E. P. *Angew. Chem., Int. Ed.* **2011**, *50*, 6530.
(7) (a) Ishikawa, N.; Sugita, M.; Wernsdorfer, W. *Angew. Chem., Int. Ed.* **2005**, *44*, 2931. (b) Ishikawa, N.; Sugita, M.; Okubo, T.; Tanaka, N.; Iino, T.; Kaizu, Y. *Inorg. Chem.* **2003**, *42*, 2440. (c) Branzoli, F.; Carretta, P.; Filibian, M.; Zoppellaro, G.; Graf, M. J.; Galan-Mascaros, J. R.; Fuhr, O.; Brink, S.; Ruben, M. *J. Am. Chem. Soc.* **2009**, *131*, 4387. (d) Ishikawa, N. *Polyhedron* **2007**, *26*, 2147.
(8) (a) Tang, J.; Hewitt, I.; Madhu, N. T.; Chastanet, G.; Wernsdorfer, W.; Anson, C. E.; Benelli, C.; Sessoli, R.; Powell, A. K. *Angew. Chem., Int. Ed.* **2006**, *45*, 1729. (b) Chibotaru, L. F.; Ungur, L.; Soncini, A. *Angew. Chem., Int. Ed.* **2008**, *47*, 4126. (c) Ungur, L.; Heuvela, W. V. d.; Chibotaru, L. F. *New J. Chem.* **2009**, *33*, 1224. (d) Luzon, J.; Bernot, K.; Hewitt, I. J.; Anson, C. E.; Powell, A. K.; Sessoli, R. *Phys. Rev. Lett.* **2008**, *100*, 247205.
(9) (a) Hussain, B.; Savard, D.; Burchell, T. J.; Wernsdorfer, W.; Murugesu, M. *Chem. Commun.* **2009**, 1100. (b) Ke, H.; Xu, G.-F.; Zhao, L.; Tang, J.; Zhang, X.-Y.; Zhang, H.-J. *Chem.—Eur. J.* **2009**, *15*, 10335. (c) Tian, H.; Guo, Y.-N.; Zhao, L.; Tang, J.; Liu, Z. *Inorg. Chem.* **2011**, *50*, 8688.
(10) Gagne, R. R.; Spiro, C. L.; Smith, T. J.; Hamann, C. A.; Thies, W. R.; Shiemke, A. K. *J. Am. Chem. Soc.* **1981**, *103*, 4073.
(11) (a) Sheldrick, G. M. *SHELXS-97, Program for Crystal Structure Solution*; University of Göttingen: Germany, 1997; (b) Sheldrick, G. M. *SHELXL-97, Program for Crystal Structure Refinement*; University of Göttingen: Germany, 1997.
(12) (a) Albrecht, M. *Chem. Rev.* **2001**, *101*, 3457. (b) Hamblin, J.; Tuna, F.; Bunce, S.; Childs, L. J.; Jackson, A.; Errington, W.; Alcock, N. W.; Nierengarten, H.; Van Dorsselaer, A.; Leize-Wagner, E.; Hannon, M. J. *Chem.—Eur. J.* **2007**, *13*, 9286.
(13) (a) Senegas, J.-M.; Koeller, S.; Bernardinelli, G.; Piguet, C. *Chem. Commun.* **2005**, 2235. (b) Ronson, T. K.; Adams, H.; Harding, L. P.; Pope, S. J. A.; Sykes, D.; Faulkner, S.; Ward, M. D. *Dalton Trans.* **2007**, 1006.
(14) Lin, S.-Y.; Xu, G.-F.; Zhao, L.; Guo, Y.-N.; Guo, Y.; Tang, J. *Dalton Trans.* **2011**, *40*, 8213.
(15) (a) Kahn, M. L.; Sutter, J.-P.; Golhen, S.; Guionneau, P.; Ouahab, L.; Kahn, O.; Chasseau, D. *J. Am. Chem. Soc.* **2000**, *122*, 3413. (b) Kahn, M. L.; Ballou, R.; Porcher, P.; Kahn, O.; Sutter, J.-P. *Chem.—Eur. J.* **2002**, *8*, 525. (c) Guo, Y.-N.; Chen, X.-H.; Xue, S.; Tang, J. *Inorg. Chem.* **2011**, *50*, 9705.
(16) Osa, S.; Kido, T.; Matsumoto, N.; Re, N.; Pochaba, A.; Mrozinski, J. *J. Am. Chem. Soc.* **2003**, *126*, 420.
(17) Bi, Y.; Guo, Y.-N.; Zhao, L.; Guo, Y.; Lin, S.-Y.; Jiang, S.-D.; Tang, J.; Wang, B.-W.; Gao, S. *Chem.—Eur. J.* **2011**, *17*, 12476.
(18) (a) Jiang, S. D.; Wang, B. W.; Su, G.; Wang, Z. M.; Gao, S. *Angew. Chem., Int. Ed.* **2010**, *49*, 7448. (b) Lin, P.-H.; Sun, W.-B.; Yu, M.-F.; Li, G.-M.; Yan, P.-F.; Murugesu, M. *Chem. Commun.* **2011**, *47*, 10993.
(19) Bartolome, J.; Filoti, G.; Kuncser, V.; Schinteie, G.; Mereacre, V.; Anson, C. E.; Powell, A. K.; Prodius, D.; Turta, C. *Phys. Rev. B* **2009**, *80*, 014430.
(20) Luis, F.; Bartolome, J.; Fernandez, J. F.; Tejada, J.; Hernandez, J. M.; Zhang, X. X.; Ziolo, R. *Phys. Rev. B* **1997**, *55*, 11448.
(21) (a) Layfield, R. A.; McDouall, J. J. W.; Sulway, S. A.; Tuna, F.; Collison, D.; Winpenny, R. E. P. *Chem.—Eur. J.* **2010**, *16*, 4442. (b) Wang, Y.; Li, X. L.; Wang, T. W.; Song, Y.; You, X. Z. *Inorg. Chem.* **2010**, *49*, 969.
(22) (a) Antunes, M. A.; Pereira, L. C. J.; Santos, I. C.; Mazzanti, M.; Marçalo, J.; Almeida, M. *Inorg. Chem.* **2011**, *50*, 9915. (b) Abbas, G.; Lan, Y.; Kostakis, G. E.; Wernsdorfer, W.; Anson, C. E.; Powell, A. K. *Inorg. Chem.* **2010**, *49*, 8067.
(23) (a) Chen, G. J.; Gao, C. Y.; Tian, J. L.; Tang, J.; Gu, W.; Liu, X.; Yan, S. P.; Liao, D. Z.; Cheng, P. *Dalton Trans.* **2011**, *40*, 5579. (b) Long, J.; Habib, F.; Lin, P. H.; Korobkov, I.; Enright, G.; Ungur, L.; Wernsdorfer, W.; Chibotaru, L. F.; Murugesu, M. *J. Am. Chem. Soc.* **2011**, *133*, 5319. (c) Zheng, Y.-Z.; Lan, Y.; Anson, C. E.; Powell, A. K. *Inorg. Chem.* **2008**, *47*, 10813.
(24) Ma, Y.; Xu, G.-F.; Yang, X.; Li, L.-C.; Tang, J.; Yan, S.-P.; Cheng, P.; Liao, D.-Z. *Chem. Commun.* **2010**, *46*, 8264.